APPLIED SCIENCES AND ENGINEERING

Toward continuous-wave operation of organic semiconductor lasers

Atula S. D. Sandanayaka,[1,2]* Toshinori Matsushima,[1,2,3] Fatima Bencheikh,[1,2] Kou Yoshida,[1] Munetomo Inoue,[1] Takashi Fujihara,[4,5] Kenichi Goushi,[1,2,3] Jean-Charles Ribierre,[1,2] Chihaya Adachi[1,2,3,4,5]*

The demonstration of continuous-wave lasing from organic semiconductor films is highly desirable for practical applications in the areas of spectroscopy, data communication, and sensing, but it still remains a challenging objective. We report low-threshold surface-emitting organic distributed feedback lasers operating in the quasi–continuous-wave regime at 80 MHz as well as under long-pulse photoexcitation of 30 ms. This outstanding performance was achieved using an organic semiconductor thin film with high optical gain, high photoluminescence quantum yield, and no triplet absorption losses at the lasing wavelength combined with a mixed-order distributed feedback grating to achieve a low lasing threshold. A simple encapsulation technique greatly reduced the laser-induced thermal degradation and suppressed the ablation of the gain medium otherwise taking place under intense continuous-wave photoexcitation. Overall, this study provides evidence that the development of a continuous-wave organic semiconductor laser technology is possible via the engineering of the gain medium and the device architecture.

INTRODUCTION

Organic semiconducting materials are generally considered to be well suited for applications in photonics because of their ability to emit, modulate, and detect light (*1*). In particular, considerable research efforts have been undertaken during the last two decades to use them in optically pumped solid-state laser sources because of their outstanding features in terms of low-cost fabrication, easy processability, chemical versatility, mechanical flexibility, and wavelength tunability across the whole visible range (*2*–*6*). Since the first demonstration of an optically pumped organic semiconductor laser (OSL) (*2*), their performance has markedly improved because of significant progress in both high-gain organic semiconducting materials and device design (*7*–*15*). Owing to recent advances in low-threshold distributed feedback (DFB) OSLs, direct optical pumping by electrically driven, nanosecond-pulsed, inorganic, light-emitting diodes was demonstrated, providing a route toward a new compact and low-cost visible laser technology (*12*, *13*). Applications based on these OSLs are currently emerging, which include the development of spectroscopic tools, data communication devices, medical diagnostics, and chemical sensors (*16*–*20*). Nevertheless, OSLs are still optically pumped by pulsed photoexcitation (with a pulse width typically varying from 100 fs to 10 ns) and driven at repetition rates (*f*) ranging from 10 Hz to 10 kHz. In this context, further breakthroughs are still required to demonstrate optically pumped OSLs operating in the continuous-wave (CW) regime and ultimately to realize an electrically pumped organic laser diode (*21*, *22*).

The operation of OSLs in the CW regime has proven to be challenging (*23*, *24*). Thermal degradation of the organic gain medium under intense long-pulse optical pumping represents a severe issue for long-term laser operation (*25*). The other important problem that needs to be overcome is related to the losses caused by the generation of long-lived triplet excitons via intersystem crossing (*26*–*29*). When organic films are optically pumped in the long-pulse regime, the accumulation of triplet excitons generally occurs, resulting in an increased absorption at the lasing wavelength due to triplet absorption (TA) and a quenching of singlet excitons due to singlet-triplet exciton annihilation (STA). To overcome these obstacles, the incorporation of triplet quenchers, such as oxygen (*30*, *31*), cyclooctatetraene (*32*), and an anthracene derivative (*33*), in organic films has been proposed. Another way to considerably reduce the triplet losses is based on the use of emitters showing a high photoluminescence quantum yield (PLQY) and no spectral overlap between the absorption band of the triplet excited states and the emission band of the singlet excited states (*34*–*36*). Both methods to suppress triplet losses in OSLs have been successfully used to improve device performance in the quasi-CW (qCW) regime (*31*, *35*). In parallel, a CW lasing duration of nearly 100 μs could be achieved in an OSL containing an anthracene derivative as triplet quencher (*33*). Herein, we propose an improved DFB OSL architecture that enables qCW lasing (at the very high repetition rate of 80 MHz) and long-pulse surface-emitting lasing with outstanding and unprecedented performance. These results represent a major advance in the field of organic photonics and open new prospects toward the development of a reliable and cost-effective, organic-based, CW, solid-state laser technology.

RESULTS

The surface-emitting OSLs fabricated in the present study used 4,4′-bis[(*N*-carbazole)styryl]biphenyl (BSBCz) in Fig. 1 as emitter (*34*). The incorporation of triplet quenchers into BSBCz films is not necessary because of extremely weak production of triplets via intersystem crossing and negligible TA at the lasing wavelength in this material (*35*). The fabrication method and the structure of the organic semiconductor

[1]Center for Organic Photonics and Electronics Research, Kyushu University, 744 Motooka, Nishi, Fukuoka 819-0395, Japan. [2]Japan Science and Technology Agency, Exploratory Research for Advanced Technology, Adachi Molecular Exciton Engineering Project, 744 Motooka, Nishi, Fukuoka 819-0395, Japan. [3]International Institute for Carbon Neutral Energy Research (WPI-I2CNER), Kyushu University, 744 Motooka, Nishi, Fukuoka 819-0395, Japan. [4]Innovative Organic Device Laboratory, Institute of Systems, Information Technologies and Nanotechnologies, 5-14 Kyudai-shinmachi, Nishi, Fukuoka 819-0388, Japan. [5]Fukuoka i[3]-Center for Organic Photonics and Electronics Research (i[3]-OPERA), 5-14 Kyudai-shinmachi, Nishi, Fukuoka 819-0388, Japan.
*Corresponding author. Email: adachi@cstf.kyushu-u.ac.jp (C.A.); sandanay@opera.kyushu-u.ac.jp (A.S.D.S.)

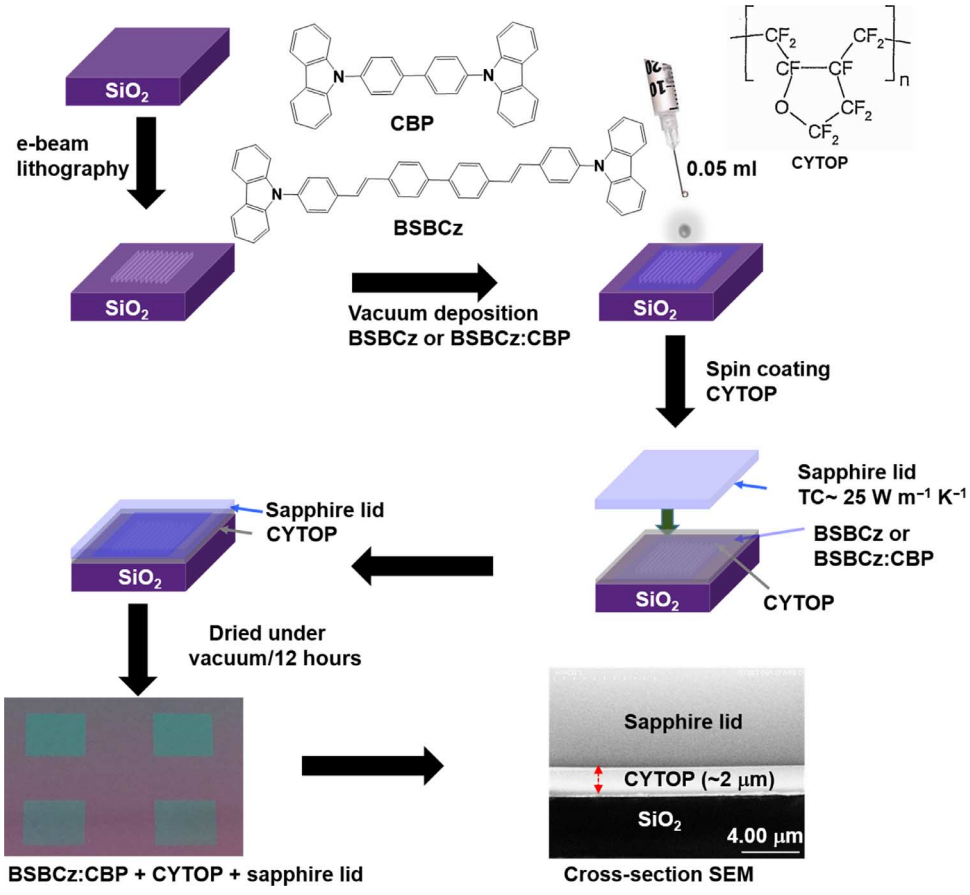

Fig. 1. Fabrication method of the organic semiconductor DFB lasers. Schematic representation of the method used to fabricate the organic DFB lasers. The different successive steps involve the fabrication of the DFB resonator structure by electron beam (e-beam) lithography, thermal evaporation of the organic semiconductor thin film, and spin coating of CYTOP polymer film followed by device sealing with a high–thermal conductivity (TC) sapphire lid.

DFB lasers fabricated in this study are schematically represented in Figs. 1 and 2A, respectively. To achieve a low lasing threshold with lasing emission in the direction normal to the substrate plane, we designed a mixed-order DFB grating architecture with second-order Bragg scattering regions surrounded by first-order scattering regions that give rise to a strong feedback, providing an efficient vertical outcoupling of the laser radiation (*8*). In a DFB structure, laser oscillation takes place when the Bragg condition $m\lambda_{Bragg} = 2n_{eff}\Lambda$ is satisfied (*5*), where m is the order of diffraction, λ_{Bragg} is the Bragg wavelength, n_{eff} is the effective refractive index of the gain medium, and Λ is the period of the grating. Using the reported n_{eff} and λ_{Bragg} values for BSBCz (*37*–*39*), the grating periods for a mixed-order ($m = 1, 2$) DFB laser device are calculated to be 140 and 280 nm, respectively. These gratings were directly engraved using electron beam lithography and reactive ion etching onto silicon dioxide surfaces over an area of 5 × 5 mm^2. Note that optical simulations and experimental data (see section S1) reported in figs. S1 and S2 and tables S1 to S3 were taken into account to choose the parameters used in the resonator design.

As shown by the scanning electron microscopy (SEM) images in Fig. 2 (B and C), the DFB gratings fabricated in this work had grating periods of 140 ± 5 and 280 ± 5 nm with a grating depth of about 65 ± 5 nm, which is in accordance with our specifications. The length of each first- and second-order DFB grating was about 15.12 and 10.08 μm, respectively. BSBCz neat films and BSBCz:CBP [6:94 weight % (wt %) and 20:80 wt %] blend films with a thickness of 200 nm were prepared on top of the gratings by vacuum deposition. As shown in Fig. 2 (D and E), the surface morphology of the organic layers presents a grating structure with a surface modulation depth of 20 to 30 nm. To greatly improve the efficiency and the stability of the DFB lasers operating in the qCW and long-pulse regimes, we then encapsulated the devices in a nitrogen-filled glove box (*40*). For this purpose, 0.05 ml of CYTOP (a chemically robust, optically transparent fluoropolymer with a refractive index of about 1.35) was directly spin-coated on top of the organic layer, and the polymer film was then covered by a transparent sapphire lid, which was chosen because of its good TC (~25 W m^{-1} K^{-1} at 300 K) and good transparency at the BSBCz lasing wavelength, to seal the organic laser devices. The CYTOP film typically had a thickness of around 2 μm and was found to not affect the photophysical properties of the BSBCz films (fig. S3).

The lasing properties of encapsulated mixed-order DFB devices using either a BSBCz neat film or a BSBCz:CBP (6:94 wt %) blend film as the gain medium were first examined under pulsed optical pumping using a nitrogen gas laser delivering 800-ps pulses at a repetition rate of 20 Hz and a wavelength of 337 nm (see section S2 and fig. S4). In the case of the CBP blend films, the excitation light was mainly absorbed by the CBP host, but the large spectral overlap between CBP emission and BSBCz absorption guaranteed an efficient Förster-type energy transfer from the host to the guest molecules (*39*). This was confirmed by the

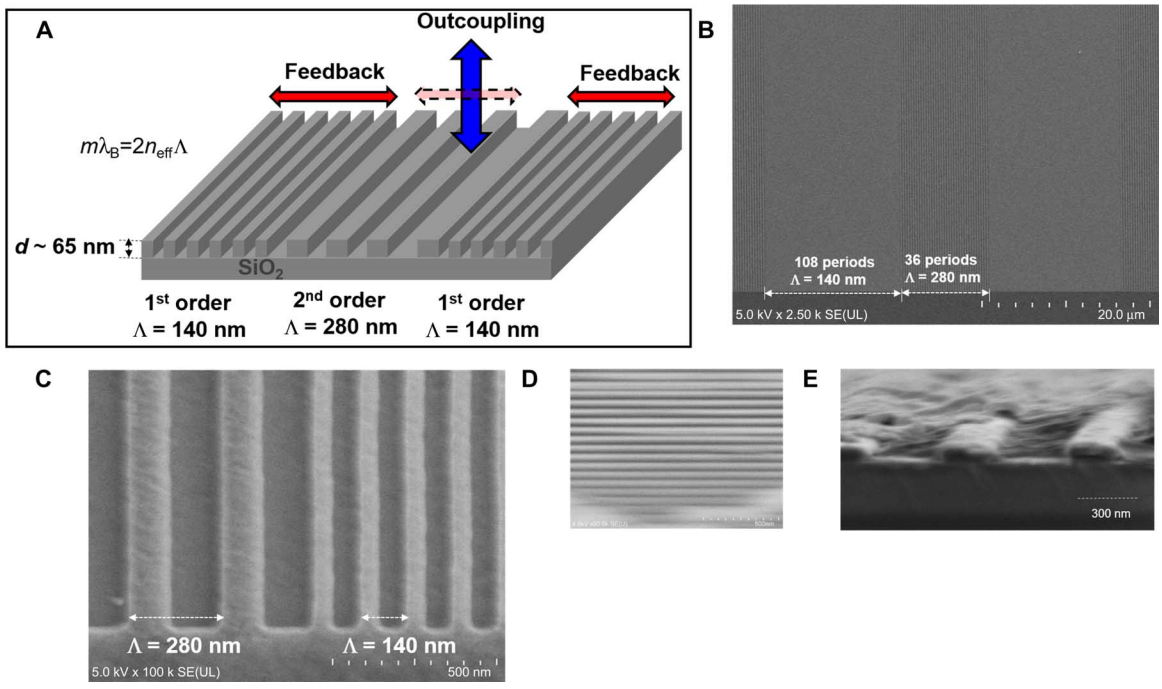

Fig. 2. Structure of the mixed-order DFB resonators. (**A**) Schematic representation of the mixed-order DFB grating structure used in this study. SEM images with (**B**) ×2500 and (**C**) ×100,000 magnification and (**D**) SEM image and (**E**) cross-sectional SEM image of the device after the deposition of a 200-nm-thick BSBCz:CBP blend film.

absence of CBP emission under 337-nm photoexcitation. On the basis of the results shown in fig. S4, the neat and blend film devices were found to exhibit low lasing thresholds of 0.22 and 0.09 μJ cm^{-2}, respectively, in the 800-ps pulse regime. In both cases, these values are lower than the previously reported thresholds for amplified spontaneous emission (ASE) (0.30 μJ cm^{-2}) (*39*) and the second-order DFB lasers (0.22 μJ cm^{-2}) (*35*) in BSBCz:CBP blends (*35*–*39*), supporting the potential of mixed-order gratings for high-performance, organic, solid-state lasers (*8*). The device encapsulation in this pulsed optical pumping regime was found to not modify the threshold and the lasing wavelength of the mixed-order DFB lasers.

qCW lasing in organic semiconductor DFB lasers

The lasing properties of various BSBCz and BSBCz:CBP (6:94 wt %) DFB devices with different resonator structures were investigated in the qCW regime using, for the optical pumping, optical pulses with a wavelength of 365 nm and a width of 10 ps from a Ti-sapphire laser. Figure 3 (A to C) shows streak camera images of the laser oscillations above threshold and the corresponding changes in emission intensities at different repetition rates in a representative encapsulated blend mixed-order DFB device. The excitation light intensity was fixed at about 0.5 μJ cm^{-2}. When increasing the repetition rate of the photoexcitation from 10 kHz to 80 MHz, the time interval between laser oscillations gradually decreased from 100 μs to 12.5 ns. For the highest repetition rates (>1 MHz), the DFB laser output emission looks continuous in the 500-μs window, indicating that the device properly worked in the qCW regime even at the highest repetition rate of 80 MHz. The possibility to operate the DFB device at such high repetition rates is related to the small TA loss and STA quenching resulting from the negligible triplet exciton formation in the BSBCz:CBP blend (*35*).

Similar experiments were performed with nonencapsulated mixed-order and second-order DFB devices based on either BSBCz neat or blend films. For each device, the laser output intensity obtained at several repetition rates was measured as a function of the excitation intensity to determine the lasing thresholds, and results for a representative encapsulated blend mixed-order DFB device at repetition rates of 10 kHz and 80 MHz are displayed in fig. S5. The repetition rate dependences of the lasing threshold in the different devices are summarized in Fig. 3D. The lasing threshold (E_{th}) was always lower in the 6 wt % blend DFB lasers essentially because of the PLQY of nearly 100% and the suppression of the concentration quenching in this gain medium (as compared with the PLQY of 76% in a BSBCz neat film) (*36*). The results also show that the lowest thresholds were obtained with the mixed-order DFB resonator structures. Noticeably, the lasing threshold for all devices only increased very slightly when the repetition rate was increased from 10 kHz to 8 MHz. Because of the absence of significant triplet accumulation in BSBCz systems (*35*), we attribute the small increase of the threshold with the repetition rate to minor degradation of the devices under high-intensity qCW irradiation (see fig. S6). The encapsulated blend mixed-order DFB laser exhibited the lowest threshold (varying from 0.06 μJ cm^{-2} at 10 kHz to 0.25 μJ cm^{-2} at 80 MHz) and was the only device operating properly at 80 MHz. When other devices were optically pumped at 80 MHz, the emission intensities very rapidly decreased, and the full width at half maximum (FWHM) values of the emission spectra detected with the streak camera before the fast degradation of the organic films were typically larger with values around 7 to 8 nm (fig. S7). This indicates that the encapsulation of the DFB devices is necessary to significantly reduce the degradation and, presumably, the laser ablation of the organic thin film taking place under high-intensity, 80-MHz photoexcitation. This reduction of the device degradation due to the encapsulation is presumably responsible for the lowering of the lasing thresholds observed in Fig. 3D.

The operational stability of the different blend DFB devices was investigated under qCW optical pumping at 8 MHz. Similar experiments

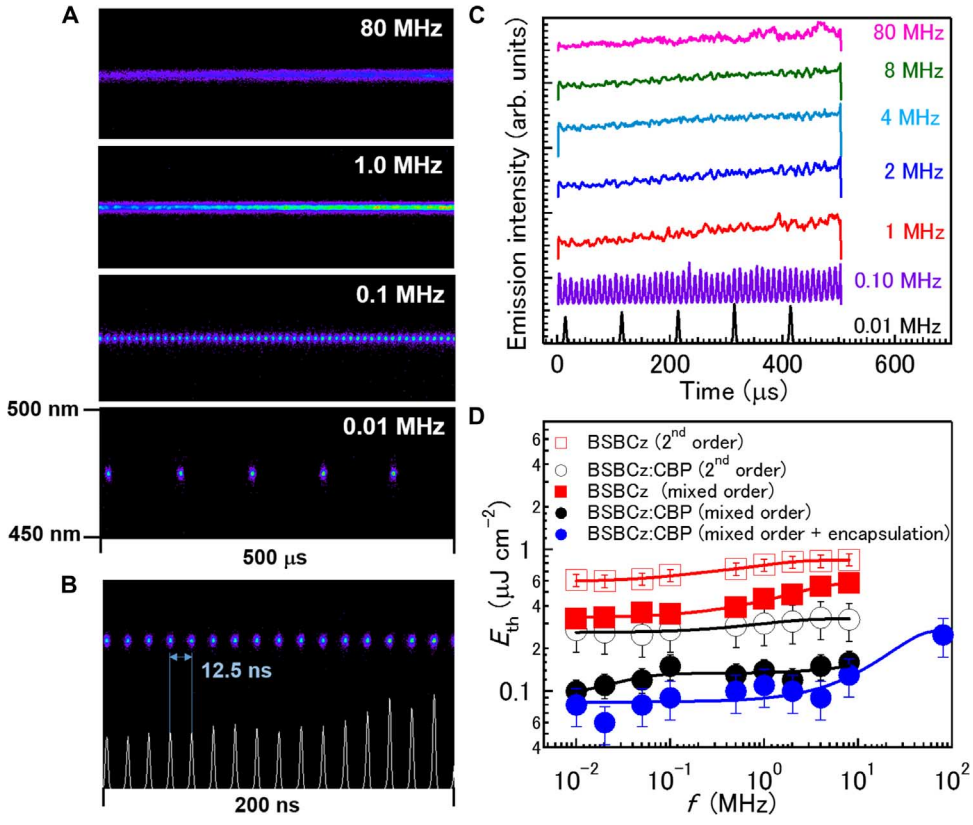

Fig. 3. Lasing properties of organic DFB lasers in the qCW regime. Streak camera images showing laser oscillations from a representative BSBCz:CBP encapsulated mixed-order DFB device at repetition rates from 0.01 to 80 MHz over a period of (**A**) 500 μs or (**B**) 200 ns (80 MHz only). Excitation intensity was fixed at ~0.5 μJ cm^{-2}, which is higher than the lasing threshold (E_{th}). (**C**) Temporal evolution of laser output intensity at various repetition rates (*f*) in an encapsulated BSBCz:CBP mixed-order DFB laser. (**D**) Lasing threshold in several types of DFB devices as a function of repetition rate. Lines serve as visual guidelines.

were also performed with the encapsulated mixed-order DFB laser at a repetition rate of 80 MHz. The temporal evolution of the different DFB laser output intensities was monitored for 20 min using a pumping intensity 1.5 times larger than the lasing threshold for each device (fig. S8). These results show that the operational stability was improved when the lasing threshold was decreased via the choice of the grating structure and the encapsulation. Higher pumping intensities were required to achieve lasing in the devices with higher threshold, which led to faster laser-induced thermal degradation. Although none of the nonencapsulated DFB devices operated well under qCW optical pumping at 80 MHz, the emission output intensity from the encapsulated organic laser after 20 min decreased to only 96% of its initial value. Such an outstanding operational stability highlights the key role played by the encapsulation on the performance of organic semiconductor DFB lasers operating in the qCW regime.

Toward CW lasing in organic semiconductor DFB lasers

The ASE properties of a 200-nm-thick BSBCz:CBP (20:80 wt %) film were investigated using the variable stripe length method to gain insights into the optical gain-and-loss coefficient under long-pulse photoirradiation. As shown in fig. S9 (see table S4 and section S3), the film optically pumped at 405 nm with 50-μs-long pulses exhibits a high net gain coefficient of 40 cm^{-1} and a loss coefficient of 3 cm^{-1} for a pumping intensity of 1.5 kW cm^{-2}. This supports our idea that BSBCz is an outstanding candidate for OSLs operating under long-pulse photoexcitation. The lasing characteristics of the DFB devices in the long-pulse regime were then investigated using an inorganic laser diode emitting at 405 nm. Because the absorption of CBP is negligible at this excitation wavelength (*30*), the concentration of BSBCz in the blend was increased to 20 wt % to improve the harvesting of the laser diode pumping emission. The PLQY of this 20 wt % blend was measured to be around 86%. Figure 4A shows the streak camera images integrated over 100 pulses of the encapsulated 20 wt % blend mixed-order DFB laser emission measured at a pumping intensity of 200 W cm^{-2} and 2.0 kW cm^{-2} for long excitation pulse widths of 800 μs and 30 ms, respectively. The corresponding emission spectra in fig. S10 provide additional evidence with the picture in Fig. 4B that the encapsulated DFB laser operates properly in the long-pulse regime with a lasing duration, which can be extended to more than 30 ms. Other data in fig. S11 provide further evidence of lasing under long-pulse photoexcitation of 30 ms. As shown in fig. S12, the DFB laser emission output intensity decreased when increasing the number of successive 30-ms-long excitation pulses from 10 to 500, which is presumably due to thermal degradation of the gain medium under such intense irradiation. Although the encapsulation of the device between high-TC silicon and sapphire improved the performance and the stability of the OSLs to an unprecedented level, this suggests that the heat dissipation will still need to be improved in the future for the development of a real CW organic laser technology. Figure S12 also shows that no quenching of singlet excitons by TA or STA occurs in BSBCz (see section S4). The results confirm the negligible overlap between the emission and the TA of BSBCz and the absence of detrimental triplet losses in the gain medium even under intense

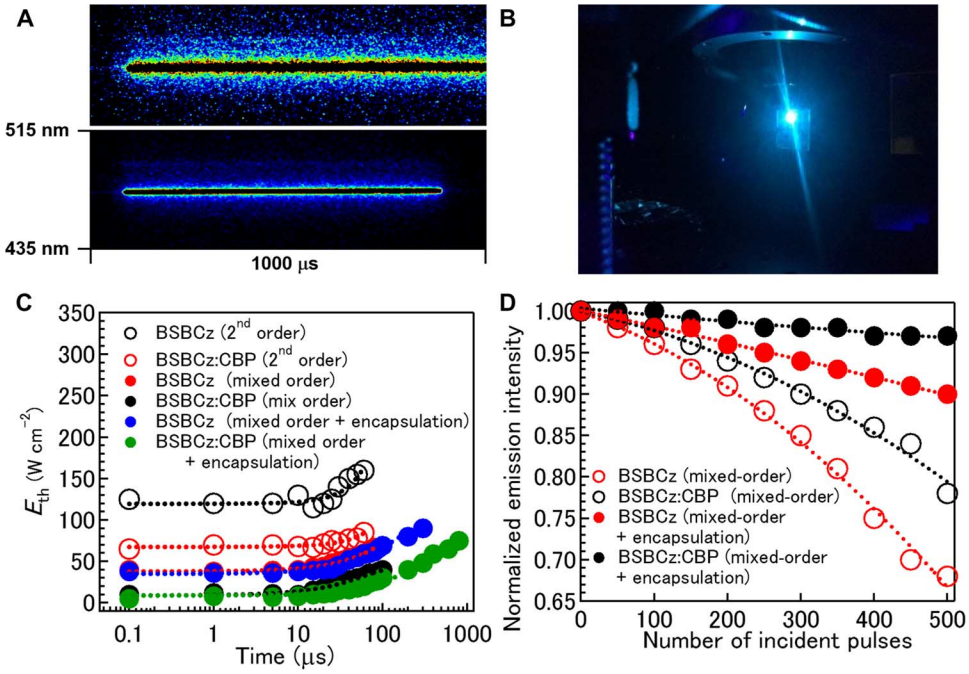

Fig. 4. Lasing properties of organic DFB lasers in the long-pulse regime. (**A**) Streak camera images showing laser emission integrated over 100 pulses from an encapsulated mixed-order DFB device using a BSBCz:CBP (20:80 wt %) film as gain medium and optically pumped by pulses of 30 ms and 2.0 kW cm^{-2} (top) or 800 μs and 200 W cm^{-2} (bottom). (**B**) Photograph of DFB device operating in the long-pulse regime (excitation, 30 ms). (**C**) Lasing threshold (E_{th}) in various DFB devices as a function of excitation duration. Dotted lines serve as visual guidelines. (**D**) Change in laser output intensity from organic DFB lasers as a function of the number of incident pulses (100 μs and 200 W cm^{-2}).

long-pulse photoexcitation (*35*). To authenticate the claim of lasing, we examined the divergence of the emitted beam below and above threshold as well as its polarization. The results displayed in figs. S13 and S14 confirm that a proper lasing operation takes place in BSBCz DFB devices under long-pulse photoirradiation.

The organic DFB laser output intensity and emission spectra were measured as a function of the excitation intensity in the devices with different structures and various long-pulse durations ranging from 0.1 to 1000 μs. An example of data obtained from a representative encapsulated blend mixed-order device is displayed in fig. S15. The abrupt change in the slope efficiency of the laser output intensity was used again to determine the lasing threshold. Figure 4C summarizes the pulse duration dependence of the laser thresholds measured in the different devices. Similar to the trends observed in the qCW regime, blending BSBCz into a CBP host using a mixed-order DFB resonator structure and encapsulating the device led to a substantial lowering of the lasing threshold. Although the BSBCz neat film–based encapsulated mixed-order DFB device could operate properly in the long-pulse regime for durations longer than 100 μs, the encapsulated blend mixed-order organic DFB laser showed the lowest lasing thresholds (range, 5 to 75 W cm^{-2}) and was the only device that could produce lasing effectively for durations longer than 800 μs. To provide additional evidence of the key role played by the choice of high-TC sapphire as encapsulation lid on the performance of the OSLs in the long-pulse regime, we compared the excitation duration dependence of the lasing thresholds obtained in the mixed-order blend DFB devices encapsulated with either a sapphire or a glass lid. Figure S16 demonstrates that the use of a high-TC lid made of sapphire leads to a lower threshold and improved operational stability.

The operational stability of the mixed-order DFB lasers with and without encapsulation was characterized in the long-pulse regime by monitoring the laser emission output intensity of these devices above the lasing threshold as a function of the number of 100-μs excitation pulses with a pump intensity of 200 W cm^{-2}. As shown in Fig. 4D, the emission intensity gradually decreased with time in all devices, and these decreases were irreversible, indicating a laser-induced thermal degradation of the organic gain media. Noticeably, the operational stability was greatly improved by the encapsulation and was the best for the encapsulated blend device. In that latter case, the laser output intensity only decreased by 3% after 500 pulses. Figure S17 shows laser microscope images of a nonencapsulated blend mixed-order DFB laser before and after irradiation by 100 incident pulses with a width of 1 ms and an excitation intensity of 200 W cm^{-2}. Although no sign of any laser-induced thermal degradation could be observed in the encapsulated device, laser ablation took place in the nonencapsulated device with an ablated depth of about 125 nm. The possibility to greatly reduce laser ablation by the proposed encapsulation technique is evidently critical for the future development of CW OSL technologies. To derive conclusions about how the present devices are limited on the way toward achieving real CW operation, we carried out thermal simulation of the heat dissipation in the devices, which is reported in figs. S18 to S22 (see table S5 and section S5). These results show the influence of the pump pulse width and the role of the encapsulation on the thermal properties of the devices. In particular, although the encapsulation has been found to be a critical element in this study, the simulation suggests that CYTOP should be replaced in further studies by another material with a better TC.

DISCUSSION

The first demonstration of an inorganic CW solid-state laser was reported about four decades ago (*41*), and the development has since been proven to be very successful, especially at wavelengths in the near-infrared

and the ultraviolet/blue regions of the electromagnetic spectrum (*42*–*45*). Although these devices generally require sophisticated microfabrication techniques with high vacuum and temperature conditions, it was recently demonstrated that CW lasing could also be achieved using solution-processed inorganic quantum wells (*46*). On the other hand, the performance of the OSLs in the qCW and long-pulse regimes has, to date, remained far below that of inorganic semiconductors (*33*, *35*).

Our demonstration of an OSL operating at 80 MHz in the qCW regime and still working in the long-pulse regime after 500 successive pulses of 30 ms thus represents a major step toward the development of a real CW, organic, solid-state laser technology. The present study strongly supports the fact that organic lasing materials with high PLQY, high optical gain, and no spectral overlap between lasing emission peak and TA bands are highly desirable for suppressing the triplet losses and, when combined with mixed-order DFB gratings, achieving low-threshold CW lasers. The results also demonstrate that the use of silicon and sapphire encapsulating lids with higher TCs (*47*) than those of conventional glass and fused silica improved the efficiency and stability of the organic DFB lasers, but laser-induced thermal degradation of the organic gain medium under intense CW optical pumping remains the most severe issue that will need to be overcome in the near future. Further work to greatly enhance the CW OSL operational stability should thus now focus on the development of organic semiconductor gain media with low CW lasing thresholds and enhanced thermal stability as well as on the integration of efficient heat dissipation systems into the devices, taking into account perhaps the previous approaches developed for improving the thermal management in CW, inorganic, solid-state lasers (*48*, *49*). In addition, aside from finding better and more efficient gain materials, further optimization of the resonator geometry and laser structure should lead to lower lasing thresholds and should still represent an important future direction for the development of a CW organic laser technology and for the realization of an electrically pumped organic laser diode.

MATERIALS AND METHODS

Device fabrication

Silicon substrates covered with a thermally grown silicon dioxide layer with a thickness of 1 μm were cleaned by ultrasonication using alkali detergent, pure water, acetone, and isopropanol followed by ultraviolet-ozone treatment. The silicon dioxide surfaces were treated with hexamethyldisilazane by spin coating at 4000 rpm for 15 s and annealed at 120°C for 120 s. A resist layer with a thickness of around 70 nm was spin-coated on the substrates at 4000 rpm for 30 s from a ZEP520A-7 solution (ZEON Co.) and baked at 180°C for 240 s. Electron beam lithography was performed to draw grating patterns on the resist layer using a JBX-5500SC system (JEOL) with an optimized dose of 0.1 nC cm^{-2}. After the electron beam irradiation, the patterns were developed in a developer solution (ZED-N50, ZEON Co.) at room temperature. The patterned resist layer was used as an etching mask while the substrate was plasma-etched with CHF_3 using an EIS-200ERT etching system (Elionix). To completely remove the resist layer from the substrate, the substrate was plasma-etched with O_2 using a FA-1EA etching system (SAMCO). The gratings formed on the silicon dioxide surfaces were observed with SEM (SU8000, Hitachi). To complete the laser devices, 6 or 20 wt % BSBCz:CBP blend films with a thickness of 200 nm and BSBCz neat films were prepared on the gratings by thermal evaporation under a pressure of 2.0×10^{-4} Pa with a total evaporation rate of 0.1 to 0.2 nm s^{-1}. Finally, 0.05 ml of CYTOP (Asahi Glass Co. Ltd.) was directly spin-coated at 1000 rpm for 30 s onto the DFB laser devices, sandwiched with sapphire lids to seal the top of the laser devices, and dried in a vacuum overnight.

Spectroscopy measurements

For the characterization of the pulsed organic lasers, pulsed excitation light from a nitrogen gas laser (USHO, KEN-2020) was focused on a 6×10^{-3}–cm^2 area of the devices through a lens and slit. The excitation wavelength was 337 nm, the pulse width was 0.8 ns, and the repetition rate was 20 Hz. The excitation light was incident upon the devices at around 20° with respect to the normal to the device plane. The emitted light was collected normal to the device surface with an optical fiber connected to a multichannel spectrometer (PMA-50, Hamamatsu Photonics) and placed 3 cm away from the device. Excitation intensities were controlled using a set of neutral density filters. For qCW operation, a mode-locked, frequency-doubled Ti-sapphire laser (Millennia Prime, Spectra-Physics) was used to generate excitation light with an excitation wavelength of 365 nm, a pulse width of 10 ps, and repetition rates ranging from 0.01 to 80 MHz. The excitation light was focused on a 1.9×10^{-4}–cm^2 area of the devices through a lens and slit, and the emitted light was collected using a streak scope (C10627, Hamamatsu Photonics) with a time resolution of 15 ps that was connected with a digital camera (C9300, Hamamatsu Photonics). For the long-pulse operation, a CW laser diode (maximum power, 1400 mW; NDV7375E, NICHIA) was used to generate excitation light with an excitation wavelength of 405 nm. In these measurements, pulses were delivered using an acousto-optic modulator (Gooch and Housego) that was triggered with a pulse generator (WF 1974, NF Co.). The excitation light was focused on a 4.5×10^{-5}–cm^2 area of the devices through a lens and slit, and the emitted light was collected using a streak scope (C7700, Hamamatsu Photonics) with a time resolution of 100 ps that was connected with a digital camera (C9300, Hamamatsu Photonics). The emission intensity was recorded using a photomultiplier tube (PMT) (C9525-02, Hamamatsu Photonics). Both the PMT response and the driving square wave signal were monitored on a multichannel oscilloscope (MSO6104A, Agilent Technologies). The same irradiation and detection angles were used for this measurement, as previously described. The size of the excitation area was carefully checked by using a beam profiler (WinCamD-LCM, DataRay). All the measurements were performed in a nitrogen atmosphere to prevent any degradation resulting from moisture and oxygen. The solution containing BSBCz in CH_2Cl_2 was prepared and bubbled with argon before use. Third-harmonic-wave laser light with a wavelength of 355 nm and a FWHM of 5 ns from a Nd:YAG laser (Quanta-Ray GCR-130, Spectra-Physics) was used as pump light, and pulsed white light from a Xe lamp was used as probe light for the TA measurement on the solution using a streak camera (C7700, Hamamatsu Photonics).

SUPPLEMENTARY MATERIALS

Supplementary material for this article is available at http://advances.sciencemag.org/cgi/content/full/3/4/e1602570/DC1

section S1. Optical simulations
section S2. Lasing properties of mixed-order DFB devices
section S3. Optical gain
section S4. Transient absorption
section S5. Thermal simulations
fig. S1. Schematic of the geometry used for optical simulation.
fig. S2. Lasing threshold of mixed-order DFB lasers based on BSBCz:CBP (6:94 wt %) 200-nm-thick film for different dimensions of the second-order gratings.
fig. S3. Photophysical properties of films with and without encapsulation.
fig. S4. Characterization of the pulsed organic lasers.

REFERENCES AND NOTES

1. J. Clark, G. Lanzani, Organic photonics for communications. *Nat. Photon.* **4**, 438–446 (2010).
2. D. Moses, High quantum efficiency luminescence from a conducting polymer in solution: A novel polymer laser dye. *Appl. Phys. Lett.* **60**, 3215–3216 (1992).
3. N. Tessler, G. J. Denton, R. H. Friend, Lasing from conjugated-polymer microcavities. *Nature* **382**, 695–697 (1996).
4. F. Hide, M. A. Díaz-García, B. J. Schwartz, M. Andersson, Q. Pei, A. J. Heeger, Semiconducting polymers: A new class of solid-state laser materials. *Science* **273**, 1833–1836 (1996).
5. I. D. W. Samuel, G. A. Turnbull, Organic semiconductor lasers. *Chem. Rev.* **107**, 1272–1295 (2007).
6. S. Chénais, S. Forget, Recent advances in solid-state organic lasers. *Polym. Int.* **61**, 390–406 (2012).
7. M. D. McGehee, A. J. Heeger, Semiconducting (conjugated) polymers as materials for solid-state lasers. *Adv. Mater.* **12**, 1655–1668 (2000).
8. C. Karnutsch, C. Pflumm, G. Heliotis, J. C. deMello, D. D. C. Bradley, J. Wang, T. Weimann, V. Haug, C. Gärtner, U. Lemmer, Improved organic semiconductor lasers based on a mixed-order distributed feedback resonator design. *Appl. Phys. Lett.* **90**, 131104 (2007).
9. G. Heliotis, R. Xia, D. D. C. Bradley, G. A. Turnbull, I. D. W. Samuel, P. Andrew, W. L. Barnes, Two-dimensional distributed feedback lasers using a broadband, red polyfluorene gain medium. *J. Appl. Phys.* **96**, 6959–6965 (2004).
10. A. E. Vasdekis, G. Tsiminis, J.-C. Ribierre, L. O'Faolain, T. F. Krauss, G. A. Turnbull, I. D. W. Samuel, Diode pumped distributed Bragg reflector lasers based on a dye-to-polymer energy transfer blend. *Opt. Express* **14**, 9211–9216 (2006).
11. J. C. Ribierre, G. Tsiminis, S. Richardson, G. A. Turnbull, I. D. W. Samuel, H. S. Barcena, P. L. Burn, Amplified spontaneous emission and lasing properties of bisfluorene-cored dendrimers. *Appl. Phys. Lett.* **91**, 081108 (2007).
12. Y. Yang, G. A. Turnbull, I. D. W. Samuel, Hybrid optoelectronics: A polymer laser pumped by a nitride light-emitting diode. *Appl. Phys. Lett.* **92**, 163306 (2008).
13. G. Tsiminis, Y. Wang, A. L. Kanibolotsky, A. R. Inigo, P. J. Skabara, I. D. W. Samuel, G. A. Turnbull, Nanoimprinted organic semiconductor lasers pumped by a light-emitting diode. *Adv. Mater.* **25**, 2826–2830 (2013).
14. E. R. Martins, Y. Wang, A. L. Kanibolotsky, P. J. Skabara, G. A. Turnbull, I. D. W. Samuel, Low-threshold nanoimprinted lasers using substructured gratings for control of distributed feedback. *Adv. Opt. Mater.* **1**, 563–566 (2013).
15. J. Herrnsdorf, Y. Wang, J. J. D. McKendry, Z. Gong, D. Massoubre, B. Guilhabert, G. Tsiminis, G. A. Tunrbull, I. D. W. Samuel, N. Laurand, E. Gu, M. D. Dawson, Micro-LED pumped polymer laser: A discussion of future pump sources for organic lasers. *Laser Photon. Rev.* **7**, 1065–1078 (2013).
16. C. Grivas, M. Pollnau, Organic solid-state integrated amplifiers and lasers. *Laser Photon. Rev.* **6**, 419–462 (2012).
17. C. Vannahme, S. Klinkhammer, U. Lemmer, T. Mappes, Plastic lab-on-a-chip for fluorescence excitation with integrated organic semiconductor lasers. *Opt. Express* **19**, 8179–8186 (2011).
18. W. Zheng, L. He, Label-free, real-time multiplexed DNA detection using fluorescent conjugated polymers. *J. Am. Chem. Soc.* **131**, 3432–3433 (2009).
19. Y. Wang, P. O. Morawska, A. L. Kanibolotsky, P. J. Skabara, G. A. Turnbull, I. D. W. Samuel, LED pumped polymer laser sensor for explosives. *Laser Photon. Rev.* **7**, L71–L76 (2013).
20. A. Rose, Z. Zhu, C. F. Madigan, T. M. Swager, V. Bulović, Sensitivity gains in chemosensing by lasing action in organic polymers. *Nature* **434**, 876–879 (2005).
21. I. D. W. Samuel, E. B. Namdas, G. A. Turnbull, How to recognize lasing. *Nat. Photon.* **3**, 546–549 (2009).
22. S. Z. Bisri, T. Takenobu, Y. Iwasa, The pursuit of electrically-driven organic semiconductor lasers. *J. Mater. Chem. C* **2**, 2827–2836 (2014).
23. R. Bornemann, E. Thiel, P. H. Bolívar, High-power solid-state cw dye laser. *Opt. Express* **19**, 26382–26393 (2011).
24. R. Bornemann, U. Lemmer, E. Thiel, Continuous-wave solid-state dye laser. *Opt. Lett.* **31**, 1669–1671 (2006).
25. Z. Zhao, O. Mhibik, T. Leang, S. Forget, S. Chénais, Thermal effects in thin-film organic solid-state lasers. *Opt. Express* **22**, 30092–30107 (2014).
26. N. C. Giebink, S. R. Forrest, Temporal response of optically pumped organic semiconductor lasers and its implication for reaching threshold under electrical excitation. *Phys. Rev. B* **79**, 073302 (2009).
27. M. A. Baldo, R. J. Holmes, S. R. Forrest, Prospects for electrically pumped organic lasers. *Phys. Rev. B* **66**, 035321 (2002).
28. M. Lehnhardt, T. Riedl, T. Weimann, W. Kowalsky, Impact of triplet absorption and triplet-singlet annihilation on the dynamics of optically pumped organic solid-state lasers. *Phys. Rev. B* **81**, 165206 (2010).
29. M. A. Stevens, C. Silva, D. M. Russell, R. H. Friend, Exciton dissociation mechanisms in the polymeric semiconductors poly(9,9-dioctylfluorene) and poly(9,9-dioctylfluorene-co-benzothiadiazole). *Phys. Rev. B* **63**, 165213 (2001).
30. L. Zhao, M. Inoue, K. Yoshida, A. S. D. Sandanayaka, J. H. Kim, J.-C. Ribierre, C. Adachi, Singlet-triplet exciton annihilation nearly suppressed in organic semiconductor laser materials using oxygen as a triplet quencher. *J. Sel. Topics Quantum Electron.* **22**, 1300209 (2016).
31. A. S. D. Sandanayaka, L. Zhao, D. Pitrat, J.-C. Mulatier, T. Matsushima, C. Andraud, J.-H. Kim, J.-C. Ribierre, C. Adachi, Improvement of the quasi-continuous-wave lasing properties in organic semiconductor lasers using oxygen as triplet quencher. *Appl. Phys. Lett.* **108**, 223301 (2016).
32. S. Schols, A. Kadashchuk, P. Heremans, A. Helfer, U. Scherf, Triplet excitation scavenging in films of conjugated polymers. *Chemphyschem* **10**, 1071–1076 (2009).
33. Y. F. Zhang, S. R. Forrest, Existence of continuous-wave threshold for organic semiconductor lasers. *Phys. Rev. B* **84**, 241301 (2011).
34. T. Rabe, K. Gerlach, T. Riedl, H.-H. Johannes, W. Kowalsky, J. Niederhofer, W. Gries, J. Wang, T. Weimann, P. Hinze, F. Galbrecht, U. Scherf, Quasi-continuous-wave operation of an organic thin-film distributed feedback laser. *Appl. Phys. Lett.* **89**, 081115 (2006).
35. A. S. D. Sandanayaka, K. Yoshida, M. Inoue, K. Goushi, J.-C. Ribierre, T. Matsushima, C. Adachi, Quasi-continuous-wave organic thin film distributed feedback laser. *Adv. Opt. Mater.* **4**, 834–839 (2016).
36. H. Nakanotani, C. Adachi, S. Watanabe, R. Katoh, Spectrally narrow emission from organic films under continuous-wave excitation. *Appl. Phys. Lett.* **90**, 231109 (2007).
37. D. Yokoyama, M. Moriwake, C. Adachi, Spectrally narrow emissions at cutoff wavelength from edges of optically and electrically pumped anisotropic organic films. *J. Appl. Phys.* **103**, 123104 (2008).
38. H. Yamamoto, T. Oyamada, H. Sasabe, C. Adachi, Amplified spontaneous emission under optical pumping from an organic semiconductor laser structure equipped with transparent carrier injection electrodes. *Appl. Phys. Lett.* **84**, 1401–1403 (2004).
39. T. Aimono, Y. Kawamura, K. Goushi, H. Yamamoto, H. Sasabe, C. Adachi, 100% fluorescence efficiency of 4,4′-bis[(*N*-carbazole)styryl]biphenyl in a solid film and the very low amplified spontaneous emission threshold. *Appl. Phys. Lett.* **86**, 071110 (2005).
40. S. Richardson, O. P. M. Gaudin, G. A. Turnbull, I. D. W. Samuel, Improved operational lifetime of semiconducting polymer lasers by encapsulation. *Appl. Phys. Lett.* **91**, 261104 (2007).
41. Z. I. Alzerov, V. M. Andreed, D. Z. Garbuzov, Y. V. Zhilyaev, E. P. Morozov, E. L. Portnoi, V. G. Trofim, Investigation of the influence of the AlAs-GaAs heterostructure parameters on the laser threshold current and the realization of continuous emission at room temperature. *Sov. Phys. Semicond.* **4**, 1573–1575 (1971).

42. M. Beck, D. Hofstetter, T. Aellen, J. Faist, U. Oesterle, M. Ilegems, E. Gini, H. Melchior, Continuous wave operation of a mid-infrared semiconductor laser at room temperature. *Science* **295**, 301–305 (2002).
43. H. Rong, R. Jones, A. Liu, O. Cohen, D. Hak, A. Fang, M. A. Paniccia, A continuous-wave Raman silicon laser. *Nature* **433**, 725–728 (2005).
44. T. Someya, R. Werner, A. Forchel, M. Catalano, R. Cingolani, Y. Arakawa, Room temperature lasing at blue wavelengths in gallium nitride microcavities. *Science* **285**, 1905–1906 (1999).
45. A. C. Tamboli, E. D. Haberer, R. Sharma, K. H. Lee, S. Nakamura, E. L. Hu, Room temperature continuous-wave lasing in GaN/InGaN microdisks. *Nat. Photon.* **1**, 61–64 (2007).
46. J. Q. Grim, S. Christodoulou, F. Di Stasio, R. Krahne, R. Cingolani, L. Manna, I. Moreels, Continuous-wave biexciton lasing at room temperature using solution-processed quantum wells. *Nat. Nanotech.* **9**, 891–895 (2014).
47. S. H. Choi, T. I. Lee, H. K. Baik, H. H. Roh, O. Kwon, D. h. Suh, The effect of electrode heat sink in organic-electronic devices. *Appl. Phys. Lett.* **93**, 183301 (2008).
48. Y. Bai, S. R. Darvish, S. Slivken, W. Zhang, A. Evans, J. Nguyen, M. Razeghi, Room temperature continuous wave operation of quantum cascade lasers with watt-level optical power. *Appl. Phys. Lett.* **92**, 101105 (2008).
49. V. Spagnolo, A. Lops, G. Scamarcio, M. S. Vitiello, C. Di Franco, Improved thermal management of mid-IR quantum cascade lasers. *J. Appl. Phys.* **103**, 043103 (2008).
50. D. Yokoyama, A. Sakaguchi, M. Suzuki, C. Adachi, Horizontal orientation of linear-shaped organic molecules having bulky substituents in neat and doped vacuum-deposited amorphous films. *Org. Electron.* **10**, 127–137 (2009).
51. S. Hirata, K. Totani, T. Yamashita, C. Adachi, M. Vacha, Large reverse saturable absorption under weak continuous incoherent light. *Nat. Mater.* **13**, 938–946 (2014).
52. S. Chenais, F. Druon, S. Forget, F. Balembois, P. Georges, On thermal effects in solid-state lasers: The case of ytterbium-doped materials. *Prog. Quantum Electron.* **30**, 89–153 (2006).

Acknowledgments: We thank W. J. Potscavage Jr. for his assistance with the preparation of this manuscript. **Funding:** This study was funded by the Japan Science and Technology Agency (ERATO, Adachi Molecular Exciton Engineering Project) under JST ERATO grant number JPMJER1305, Japan. **Author contributions:** A.S.D.S., T.M., J.-C.R., and C.A. conceived the project and the experiments. A.S.D.S., K.Y., and T.M. designed the architecture of the encapsulated devices and fabricated the DFB lasers. F.B. performed the thermal and optical simulations. A.S.D.S. carried out the SEM measurement, DFB laser characterization, optical absorption and photoluminescence measurements, and their data analysis. A.S.D.S., K.G., and T.F. carried out the qCW measurement, transient absorption measurement, and data analysis. A.S.D.S., M.I., T.F., and K.G. carried out the CW measurement and data analysis. A.S.D.S. and J.-C.R. carried out the optical gain, divergence, and polarization measurement of DFB laser emission. A.S.D.S., T.M., J.-C.R., and C.A. wrote the manuscript. K.G. helped in editing the paper. All authors discussed the results and commented on the manuscript.
Competing interests: A.S.D.S., C.A., T.M., K.Y., J.-C.R., and F.B. have patents related to the described work: Japan (2017-17936, 2017.2.2) and Korea (10-2017-0027963). The authors declare that they have no other competing interests. **Data and materials availability:** All data needed to evaluate the conclusions in the paper are present in the paper and/or the Supplementary Materials. Additional data related to this paper may be requested from the authors.

Submitted 19 October 2016
Accepted 1 March 2017
Published 28 April 2017
10.1126/sciadv.1602570

Citation: A. S. D. Sandanayaka, T. Matsushima, F. Bencheikh, K. Yoshida, M. Inoue, T. Fujihara, K. Goushi, J.-C. Ribierre, C. Adachi, Toward continuous-wave operation of organic semiconductor lasers. *Sci. Adv.* **3**, e1602570 (2017).

Toward continuous-wave operation of organic semiconductor lasers

Atula S. D. Sandanayaka, Toshinori Matsushima, Fatima Bencheikh, Kou Yoshida, Munetomo Inoue, Takashi Fujihara, Kenichi Goushi, Jean-Charles Ribierre and Chihaya Adachi

Sci Adv **3** (4), e1602570.
DOI: 10.1126/sciadv.1602570